JCI insight

RESEARCH ARTICLE

Regulation of murine NK cell exhaustion through the activation of the DNA damage repair pathway

Maite Alvarez,[1] Federico Simonetta,[1] Jeanette Baker,[1] Antonio Pierini,[1] Arielle S. Wenokur,[1] Alyssa R. Morrison,[1] William J. Murphy,[2] and Robert S. Negrin[1]

[1]Blood and Marrow Transplantation, Stanford University School of Medicine, Stanford, California, USA. [2]Department of Dermatology and Internal Medicine, University of California, Davis, Sacramento, California, USA.

NK cell exhaustion (NCE) due to sustained proliferation results in impaired NK cell function with loss of cytokine production and lytic activity. Using murine models of chronic NK cell stimulation, we have identified a phenotypic signature of NCE, characterized by upregulation of the terminal differentiation marker KLRG1 and by downregulation of eomesodermin and the activating receptor NKG2D. Chronic stimulation of mice lacking NKG2D resulted in minimal NCE compared with control mice, thus identifying NKG2D as a crucial mediator of NCE. NKG2D internalization and downregulation on NK cells have been previously observed in the presence of tumor cells with high expression of NKG2D ligands (NKG2DL) due to the activation of the DNA damage repair pathways. Interestingly, our study revealed that during NK cell activation, there is an increase of MULT1, an NKG2DL, that correlates with an induction of DNA damage. Treatment with the ATM DNA damage repair pathway inhibitor KU55933 (KU) during activation reduced NCE by improving expression of activation markers and genes involved in cell survival, through sustaining NKG2D expression and preserving cell functionality. Importantly, NK cells expanded ex vivo in the presence of KU displayed increased antitumor efficacy in both NKG2D-dependent and -independent mouse models. Collectively, these data demonstrate that NCE is caused by DNA damage and is regulated, at least in part, by NKG2D. Further, the prevention of NCE is a promising strategy to improve NK cell–based immunotherapy.

Introduction

NK cells are immunological effector cells capable of providing defense against viral infections and tumor cells without prior sensitization in a MHC-unrestricted manner (1). NK cell–based immunotherapy has been explored in multiple clinical settings. The adoptive transfer of NK cells after ex vivo activation has proven to be safe and well tolerated in patients with leukemia and lymphoma, among other cancers, resulting in the expansion of NK cells (1). Additionally, NK cells can protect from graft-versus-host disease after allogeneic hematopoietic cell transplantation (HCT) by controlling alloreactive T cells (2). However, despite these attractive qualities of NK cells, the clinical experience to date has been rather disappointing with respect to clinical outcomes, due at least in part to impaired NK cell function observed in multiple cancer settings (3–6).

We have previously shown that tumor-induced NK cell dysfunction was caused by exhaustion due to profound proliferation of NK cells and was characterized by a marked downregulation of the activating T-box transcription factors (TFs) eomesodermin (Eomes) and T-bet (7). The expression of Eomes and T-bet is important for T and NK cell maturation, differentiation, and function (8). Low expression of these TFs has been found during aging and exhaustion (7, 9). Similar to T cell exhaustion, high levels of expression of PD1 (10, 11) and/or Tim3 (6) have also been correlated with NK cell exhaustion (NCE) in humans. Interestingly, downregulation of multiple activating receptors, such as NKG2D, has also been described during exhaustion (7, 12) and with defective NK cell function (5, 13–15). However, the mechanisms that underlie these effects and regulate NK function and exhaustion are still unknown. In recent years, immune effector cell exhaustion is being increasingly recognized as a cause of dysfunction, not only in cancer (7, 16), but also in other scenarios, such as during allogeneic HCT (17) or continued IL-15 stimulation of

Conflict of interest: The authors have declared that no conflict of interest exists.

Submitted: January 25, 2019
Accepted: June 13, 2019
Published: July 25, 2019.

Reference information: *JCI Insight*. 2019;4(14):e127729. https://doi.org/10.1172/jci.insight.127729.

transplanted patients (18), with a possible consequent effect on NK cell–based immunotherapy. Curiously, impaired NK cell function has also been described during chronic viral infections (11, 19), which could be related to exhaustion as well.

In this study, we explored the effect of chronic stimulation during NK cell activation and exhaustion and evaluated the mechanisms that regulate this process in order to phenotypically characterize NCE, understand underlying mechanisms, and reverse NCE to augment NK cell function.

Results

Characterization of NCE phenotype. In order to explore the mechanisms involved in NCE, we first analyzed if sustained IL-15 stimulation was responsible for the induction of exhaustion, as a defect on NK cell function had been already reported following prolonged exposure to this cytokine (12) and in patients after transplantation (18). Phenotypically, NK cells that were exposed to chronic IL-15 displayed a significant decrease of the TF Eomes, whose downregulation has been previously linked to exhaustion (7), along with downregulation of activating receptors (NKG2D, DNAM1, TRAIL, FasL), but maintained high levels of the inhibitory receptors NKG2A and CD96 but not TIGIT (Figure 1A) when compared with acutely stimulated NK cells. Other markers for activation (Thy1.2 and Ly49G2) were downregulated as well (Figure 1A). Interestingly, the killer cell lectin-like receptor G1 (KLRG1), a terminal differentiation marker previously reported to be associated with senescence and exhaustion on T cells (20), was upregulated (Figure 1A). In contrast to what was previously reported for T cell exhaustion, PD1 was barely detected on NK cells, and the percentage of Tim3 was reduced upon chronic stimulation. As expected, these NK cells also had reduced proliferative capacities, measured by the level of expression of BCL2 and Ki67 (Figure 1, A and B). Chronic exposure to IL-15 also resulted in lower lysis of the NK-sensitive cell line Yac1 by NK cells (Figure 1C) and a reduction in the ability of NK cells to produce IFN-γ upon NK1.1 stimulation (Figure 1D), resulting in overall limited functionality as previously reported (12).

We next evaluated the effect of in vivo chronic stimulation with IL-2 or Poly I:C, directly or indirectly activating NK cells, respectively, on NCE to be able to demonstrate that any type of chronic stimulation results in the induction of NCE. Furthermore, Poly I:C, a known ligand for TLR-3, was used as a model to mimic viral infection (21). Both models showed similar results obtained with the IL-15 model (Figure 1), regarding the NK cell phenotype and functionality (Supplemental Figure 2, A–C; supplemental material available online with this article; https://doi.org/10.1172/jci.insight.127729DS1). A reduction of inflammatory cytokines in the serum of chronically treated groups was also observed in some, if not all, of the models evaluated; among these, IFN-γ was a cytokine that was downregulated in all of them (Supplemental Figure 2D). Noticeably, chronic stimulation also caused an increase of the immature-like NK cell subset ($CD27^+CD11b^-$) in the BM that could justify the consistent reduction of total numbers of splenic NK cells observed in all the models (Supplemental Figure 3, A and B) and suggest a reduced ability of NK cells to respond to stimuli and/or increased cell death. The lack of response to cytokine stimulation after chronic exposure in the models evaluated was not explained by changes in the expression of IL-2 receptor β (IL2Rβ), an important component in the signaling through IL-2 and IL-15, as others have also reported (ref. 18 and Supplemental Figure 3C).

In order to identify an exhaustion phenotypic signature, we then analyzed the data originating from the 3 different in vivo models using principal component analysis (PCA; Figure 1, E and F). PC1 was able to efficiently separate acutely stimulated murine NK cells from control mice (control and resolved groups) and was highly influenced by levels of expression of activation markers, such as Thy1.2, and inhibitory and activating receptors, such as DNAM1 or TIGIT (Figure 1, E and G). Conversely, PC2 provided a better separation between the chronically and acutely stimulated groups. As shown in Figure 1, E and G, Eomes and NKG2D downregulation and KLRG1 and NKG2A upregulation upon chronic stimulation were major factors segregating mice and conditions along the PC2 axis. The variability in the expression of other activating and inhibitory receptors between the models, such as with DNAM1 (Figure 1A and Supplemental Figure 2A), TIGIT (Supplemental Figure 4, A and B), Tim3 (Supplemental Figure 4, C and D), or PD1 (Supplemental Figure 4, E and F), did not account for the results obtained in the PCA, whereas the changing patterns of NKG2D (Figure 1A; Supplemental Figure 2A; and Supplemental Figure 4, G and H), Eomes, KLRG1, and NKG2A (Figure 1A and Supplemental Figure 2A) were similar in all the models. These data also suggest that changes of the expression of these markers are more suitable in identifying exhaustion across models.

To validate this phenotypic signature, we used a more physiological model of chronic MCMV infection. Because MCMV infection is typically cleared from spleen and liver within the first 2 weeks after viral induction/infection (22, 23), we performed phenotypical and functional analyses of NK cells that were present on the salivary glands, a site where the infection has been reported to persist for months (Supplemental Figure 5) and where there is not NK development or recruitment from the periphery, unlike in the spleen (24). As the infection progressed chronically, a reduction of the proliferative marker Ki67 was observed (Figure 2, A and B). IFN-γ production upon NK1.1 stimulation as well as the total percentage of NK cells expressing granzyme B was significantly diminished at later time points of infection (Figure 2, C–F). Additionally, the NCE signature during chronic infection identified in the previous Poly I:C model was recapitulated in this model with downregulation of Eomes, NKG2D, and Ly4G2 (Figure 2, G–I), contrasting with upregulation of KLRG1 (Figure 2J) and NKG2A (Supplemental Figure 5, A and B) when compared with the acute infection groups (3–7 days after infection). Unlike the other models, NK cells from the salivary gland significantly increased the expression of the exhaustion marker PD1 during the acute infection phase, but the expression declined at later time points, similar to the effect seen for Tim3 (Supplemental Figure 5, C and D). In the spleen, as the virus undergoes elimination (Supplemental Figure 5E), the reduction of proliferation, function, and activation observed could be associated with the previously reported contraction phase, and thus a difference cannot be made between a phenomenon of exhaustion or de novo reconstitution of NK cells at the latest point of analysis (Supplemental Figure 5, F–M, and refs. 22, 23). Still, the Ly49H activation marker, which recognize m157 glycoprotein on MCMV-infected cells, responded more strongly to MCMV infection as expected (Supplemental Figure 5, G–M). Unfortunately, Ly49H could not be evaluated in the salivary gland due to the effect of this organ-processing protocol (Supplemental Figure 5, F and G, and ref. 25).

Given the broad presence of the NCE signature in chronically stimulated NK cells, we hypothesized that this signature could also be present on in vitro models when NK cells are exposed to stimuli for long periods of time. In fact, long-term in vitro NK cell activation with IL-2 (from 7–9 days) mimicked the phenotypic NK cell profile observed during chronic in vivo IL-2 stimulation, except for NKG2A, whose expression was not upregulated unlike in the in vivo model (Supplemental Figure 6). Additionally, similar to the in vivo model (Supplemental Figure 2, B and D), further stimulation of these cells with NK1.1 resulted in a downregulation of IFN-γ and TNF-α when compared with acutely stimulated NK cells (day 4 of activation), leading to a lower expression level similar to that of resting NK cells (day 0). Importantly, stimulation of chronically IL-2–activated NK (IL-2–aNK) cells through CD16 also caused a similar pattern of IFN-γ and TNF-α downregulation (Supplemental Figure 6H). Furthermore, NK cell lytic capacities were negatively affected after long-term IL-2 activation as well (Supplemental Figure 6I), together largely proving a functional defect in chronically stimulated NK cells.

Overall, these data demonstrate that any condition that results in prolonged NK cell stimulation leads to NCE with a marked loss of function associated with reduced proliferative potential, downregulation of activation markers, and upregulation of KLRG1; therefore, exhaustion is efficiently identified by the expression of Eomes, NKG2D, and KLRG1.

Role of NKG2D in the induction of NCE after chronic stimulation. Because NKG2D downregulation was consistently observed in all of the models studied (Supplemental Figure 4, G and H), and because its role in NCE was indicated by the PCA analysis (Figure 1, E and G), the role of NKG2D on the induction of exhaustion after chronic IL-2 stimulation was assessed. While NKG2D impairment, either from genetic deletion using NKG2D-KO mice or through blockade with anti-NKG2D, did not affect the response to IL-2 during acute stimulation, it did result in a diminished NCE profile during chronic stimulation. The absence of NKG2D during chronic stimulation improved NK cell function compared with control-treated mice, measured by IFN-γ production upon NK1.1 stimulation (Figure 3A) and Yac1 tumor lysis (Figure 3B). We observed, as previously reported, a reduced killing of Yac1 by NKG2D-KO NK cells during acute stimulation due to the expression of the NKG2DL H60 by Yac1 (7), but some degree of Yac1 lysis still occurred in a NKG2D-independent manner. Importantly, NKG2D-deficient NK cells exposed to chronic IL-2 were able to maintain the level of Yac1 lysis, unlike control NK cells, suggesting that these NK cells have higher functionality mediated by MHC-I mismatch and upregulation of other activating receptors.

Indeed, when the phenotype of these cells was analyzed, upregulation of Eomes, Thy1.2 and Ly49G2 (used as substitutes for NKG2D), along with a decrease of KLRG1 compared with WT/IgG control counterparts (Figure 3, C–F) were observed, suggesting a reduction in the exhaustion phenotype. Notably, a

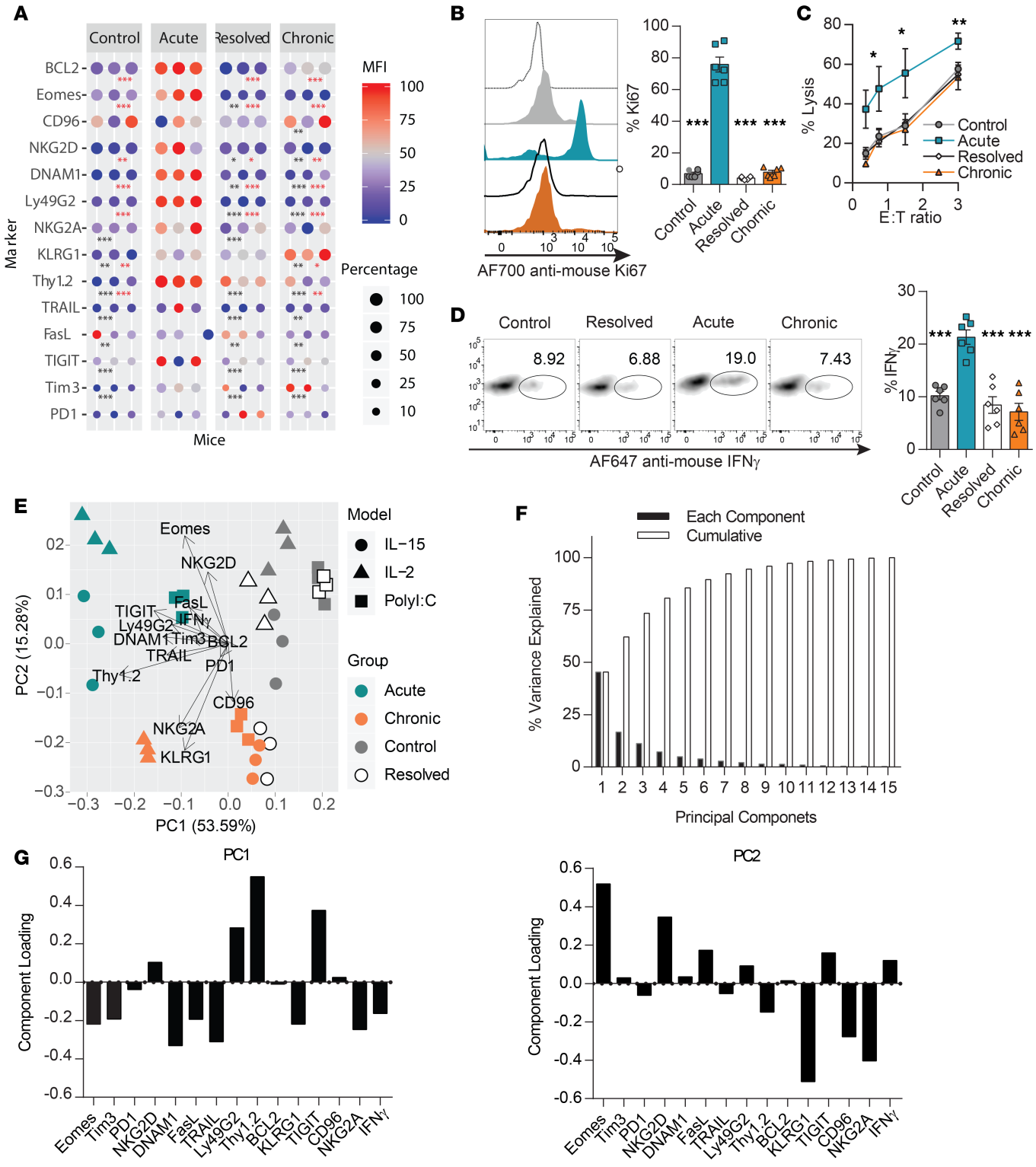

Figure 1. Exhaustion markers can be identified by changes in NK cell activation phenotype and function following chronic stimulation. Mice were treated with IL-15, as described in Supplemental Figure 1A. Spleens were collected at the indicated times and NK cells were analyzed. (**A**) Multivariate heatmap analysis was performed on data obtained from flow cytometry analysis. The percentage of a given marker within the total NK cell population is represented by the geometric size of the circle, while the color gradient represents the median fluoresce intensity (MFI) for each marker in each model representing the maximal and minimal expression within each specific marker. Statistical differences are represented in black for percentage and in red for MFI compared with the acute group. (**B**) Representative histograms and the total percentage of Ki67 on gated NK cells ($CD3^-NK1.1^+$) are shown. (**C**) The percentage of NK cell lysis of CFSE-labeled Yac1 cells is shown. The effector/target (E/T) ratio is normalized to the percentage of splenic NK cells. (**D**) Representative dot plots and the total percentage of IFN-γ production by NK cells ($CD3^-CD49b^+$) after NK1.1 stimulation are shown. (**E**) Principal component analysis (PCA) representation of NK cell markers for IL-15 (circle), IL-2 (triangle), or Poly I:C (square) models after control (gray), resolved (white), acute (turquoise), or chronic (orange) stimulation.

(**F**) The percentage of the variance for each or cumulative PC is shown. (**G**) Representation of the NK cell markers that drive PC1 and PC2 is shown. Data are representative of at least 3 independent experiments with 3 mice per group (mean ± SEM). One-way ANOVA or two-way ANOVA was used to assess significance. Significant differences are displayed for comparisons with the acute group (*$P < 0.05$, **$P < 0.01$, ***$P < 0.001$). No significant differences were found when comparisons among the control, resolved, and chronic groups were made.

decrease of the total number of NK cells was not observed between acutely and chronically IL-2–stimulated groups in NKG2D-deficient or anti-NKG2D–treated mice, unlike their corresponding controls (Supplemental Figure 7A). In contrast, the response to IL-2 by $CD8^+$ (cytotoxic) T cells was not affected by the absence of NKG2D (Supplemental Figure 7B). Although not significant, a slight increase of DNAM1- and FasL-activating receptors, but not the CD96, TIGIT, or NKG2A inhibitory receptors, was also observed in NK cells from chronically stimulated NKG2D-deficient mice when compared with controls (Supplemental Figure 7, C and D). Interestingly, an increase of activating cytokines, such as IFN-γ, TNF-α, CCL2, CCL3, and CXCL10, was detected in the serum of chronically stimulated anti-NKG2D–treated mice when compared with controls (Supplemental Figure 7E), an increase that could not be associated with $CD8^+$ T cells (Supplemental Figure 7B). On the other hand, long-term in vitro activation of NKG2D-deficient NK cells, although to a lesser extent than that in the in vivo model, resulted in a milder exhaustion phenotype with a significantly higher percentage of the activation marker Thy1.2 and reduced expression of KLRG1 (Supplemental Figure 8).

These data, therefore, indicate that NKG2D has a role in the development of exhaustion during chronic stimulation. Actually, in vitro analysis by flow cytometry and immunofluorescence revealed that NKG2D was internalized during chronic stimulation, resulting in downregulation on the surface (Figure 4).

Role of the DNA damage pathways in NCE. NKG2D internalization has been previously described in cancer patients' NK cells, due to the binding of MHC class-I–like stress molecules (NKG2DLs; refs. 5, 13, 14). Interestingly, several studies have shown that tumor cells upregulate NKG2DLs due to genotoxic and cellular stress (26). The expression of these stress molecules can indeed regulate NKG2D levels and affect function (15). Given our results regarding NKG2D internalization and downregulation and the high levels of Ki67 observed during early NK cell activation, we analyzed the level of expression of mouse NKG2DL MULT1 and Rae-1δ on NK cells during sustained in vitro stimulation. Only MULT1 was significantly increased during long-term in vitro IL-2 stimulation (Figure 5, A–C). Interestingly, the upregulation of MULT1 temporally correlated with the downregulation of NKG2D, suggesting a contribution to NKG2D loss during chronic stimulation. However, unlike NKG2D, no MULT1 internalization was detected by flow cytometry or immunofluorescence. In correlation with this data, a significant increase of the percentage of MULT1 on NK cells during acute and chronic in vivo IL-2 stimulation (Figure 5D, left) and on NK cells from the salivary gland during chronic in vivo MCMV infection (Figure 5D, right) was observed. Furthermore, blocking MULT1 in vitro caused a slight reduction of the NCE phenotype on NK cells collected at day 9 after activation (Figure 5E).

Many reports have shown that genotoxic and cellular stress cause the activation of the PI3-kinase–related protein kinases ataxia telangiectasia mutated (ATM) DNA damage repair pathway (26). Indeed, inhibition of this pathway was able to reduce the levels of NKG2DLs on tumor cells (26) or antigen-activated T cells (27). Taking into consideration the resemblance between tumor cells during uncontrolled growth and NK cells during prolonged activation, we analyzed the level of phosphorylation of ATM (pATM) during in vitro NK cell activation as an indicator of DNA damage and observed a significant increase of pATM during NK cell activation (Figure 5, F and G). Additionally, we also observed an increase in the expression of PVR on NK cells in both in vitro (Figure 5H) and in vivo exhaustion models (Figure 5I). PVR (CD155) is another stress molecule and ligand of CD96, TIGIT, and DNAM1 that has shown to be upregulated through ATM-mediated DNA damage repair pathways (28). These data suggest that DNA damage does indeed happen during NK cell activation.

In order to evaluate the role of DNA damage in the induction of NCE, the ATM DNA damage pathway was inhibited with the specific inhibitor KU55933 (KU) during the acute in vitro IL-2 activation phase (day 4), and NK cells were analyzed at later time points. The efficacy of KU treatment was confirmed by an accumulation of pATM and a reduction of phosphorylation of the ATM-dependent protein Chk2 (Supplemental Figure 9A). Conversely, the percentage of MULT1 on NK cells was not affected by KU treatment (Supplemental Figure 9B). However, significant decreases in the MFI and the mRNA expression for MULT1 were observed after KU treatment (Supplemental Figure 9B). More importantly, KU treatment did result in the maintenance

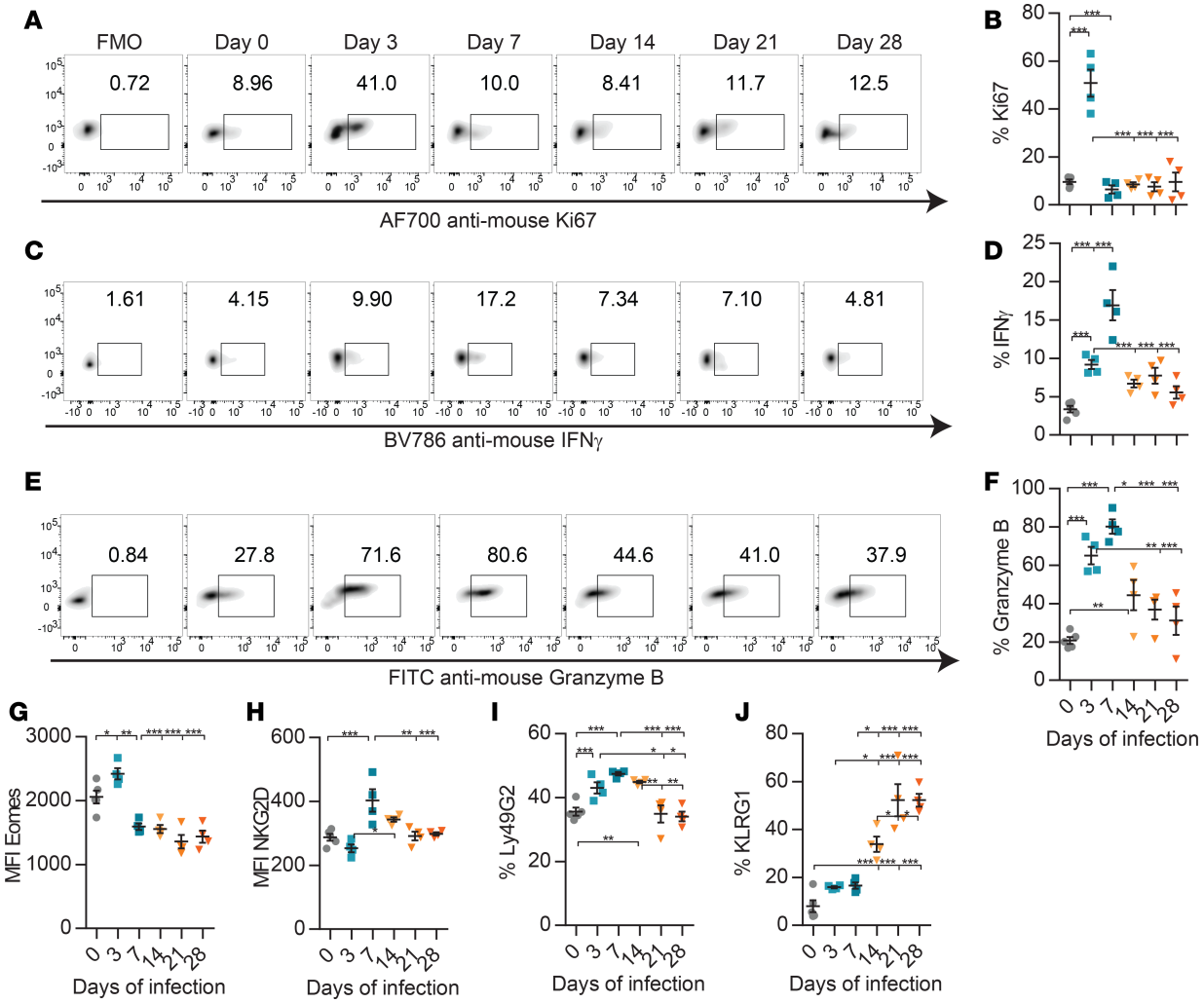

Figure 2. NK cells exposed to chronic MCMV display an exhausted phenotype. Mice were infected with MCMV for 3, 7, 14, 21, or 28 days, and salivary glands were obtained for analysis of NK cell phenotype by flow cytometry. Control unstimulated groups (gray) are represented on day 0 of infection, acute simulation groups (turquoise) on days 3 and 7, and chronic stimulation groups (orange) on days 14, 21 and 28. For IFN-γ, NK cells were stimulated with anti-NK1.1 for 4 hours before analysis. (**A**–**F**) Representative histograms or dot plots and the percentage of total expression of Ki67 (**A** and **B**), IFN-γ (**C** and **D**), and granzyme B (**E** and **F**) are shown for splenic NK cells ($CD3^-NK1.1^+$ or $CD3^-CD49d^+$). (**G**–**J**) Total MFI or percentage is shown for Eomes (**G**), NKG2D (**H**), Ly49G2 (**I**), and KLRG1 (**J**) on salivary gland–derived gated NK cells. Data are representative of 3 experiments, with 4–5 mice per group (mean ± SEM). One-way ANOVA was used to assess significance (*$P < 0.05$, **$P < 0.01$, ***$P < 0.001$).

of the NK cell activation phenotype and NK cell function for a prolonged period, delaying exhaustion (Figure 6). Indeed, unsupervised hierarchical clustering based on phenotypic characteristics revealed that NK cells collected at day 7 of activation after KU treatment clustered closer to the cells collected at day 4 during the peak of activation, compared with vehicle control–treated NK cells (Figure 6A). There were changes on the NCE signature markers that correlated with a reduction in the exhaustion phenotype, with a significant increase of Eomes (MFI) and the percentage of NKG2D as well as a decrease of percentage of KLRG1 on KU-treated NK cells (Figure 6B). Immunofluorescence analysis also demonstrated that NKG2D internalization was significantly reduced after KU treatment without affecting MULT1 expression (Supplemental Figure 9, C and D).

To identify the changes at a molecular level after KU treatment, we performed a microarray analysis on the in vitro IL-2 model (Supplemental Figure 10). Unfortunately, there were no differences in the gene expression of NK cells collected at day 9 after in vitro IL-2 stimulation when compared control- and KU-treated NK cells. However, there were a total of 901, 660, and 591 genes that were significantly upregulated (FDR ≤0.1) on NK cells collected on day 4 (acute phase), day 9 (chronic phase), and KU-treated day 9, respectively, in comparison with unstimulated NK cells from day 0 (Supplemental Figure 10, A and B). We used Ingenuity Pathway Analysis (IPA) to predict the biological processes that would be significantly

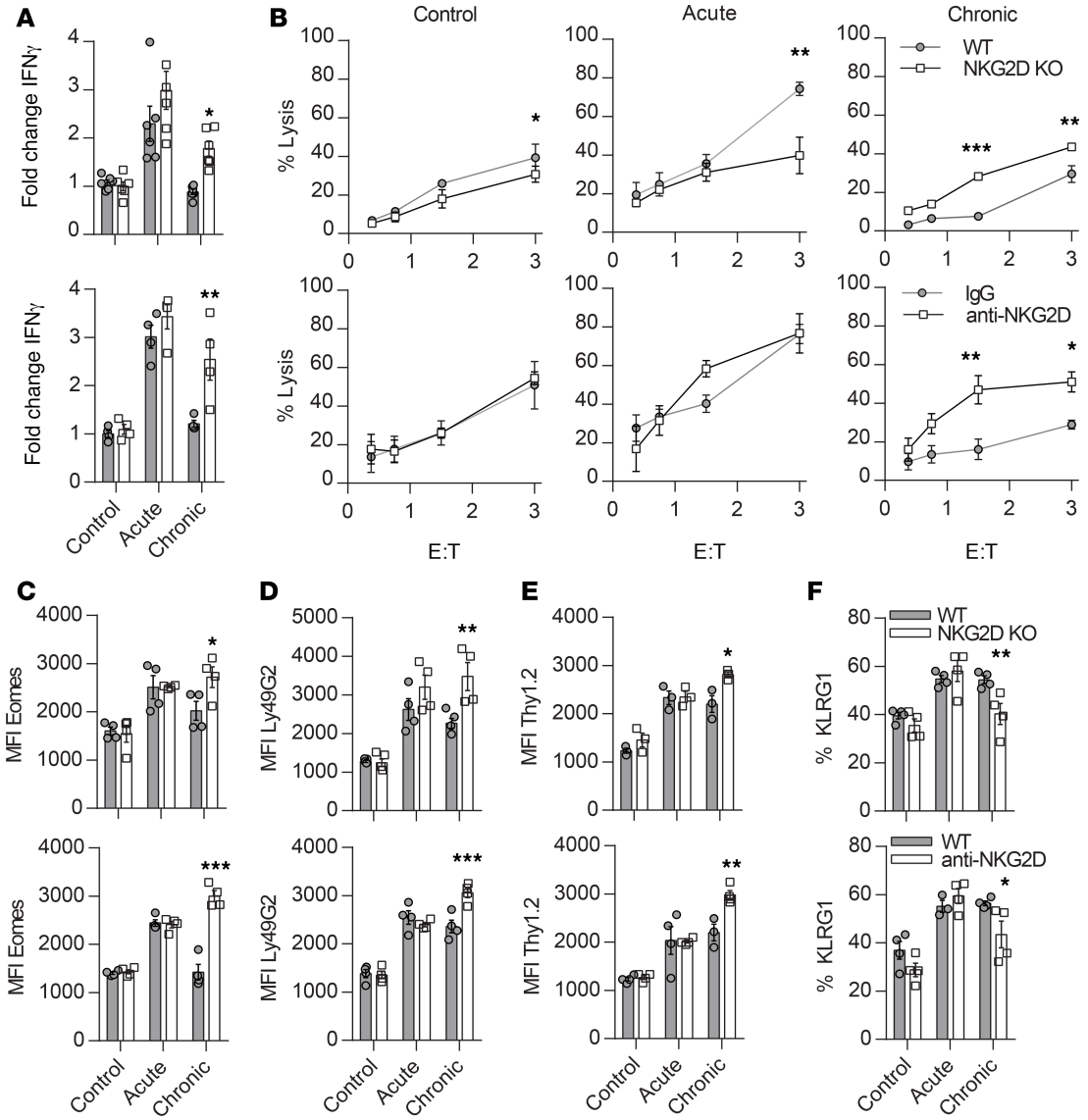

Figure 3. NKG2D deficiency during in vivo chronic IL-2 stimulation improves function and reduces NCE. WT and NKG2D-KO (top) or 200 μg IgG-treated and anti-NKG2D–treated (bottom) mice underwent chronic IL-2 in vivo stimulation, as described in Supplemental Figure 1B. (**A**) Fold change difference for the total percentage of IFN-γ production is shown for gated NK cells after NK1.1 stimulation. (**B**) The percentage of tumor lysis at different E/T ratios normalized to the percentage of NK cells during IL-2 stimulation is shown. (**C–F**) MFI or total percentage of Eomes (**C**), Ly49G2 (**D**), Thy1.2 (**E**), and KLRG1 (**F**) on gated NK cells is shown. Data are representative of at least 2 independent experiments with 4 mice per group (mean ± SEM). Significant differences are displayed for comparisons with control (WT or IgG) animals (*$P < 0.05$, **$P < 0.01$, ***$P < 0.001$).

affected from these upregulated genes. Concomitantly, IPA showed that only KU-treated NK cells had a group of upregulated genes that were significantly involved in the decrease of apoptosis ($z = –2.108$) and a group of genes involved in NK cell cytotoxicity ($z = 2.162$; Supplemental Figure 10C). In accordance with these data, KU treatment significantly increased the percentage of Ki67 and the MFI of the antiapoptotic protein BCL2 on NK cells (Figure 6, C and D), suggesting higher proliferative potential and survival capacities, respectively. BCL2 expression is regulated by the TF NF-κB, whose nuclear translocation requires proteasome function. When 20S proteasome activity was measured during NK cell activation, a decline in function was observed at later time points, while KU treatment preserved proteasome activity (Figure 6E). More importantly, KU treatment prolonged NK cell function after sustained stimulation with a significant increase of IFN-γ production and lytic capacities in KU-treated versus control NK cells (Figure 6, F and G).

To evaluate the functional effect of targeting exhaustion, the in vivo antitumor efficacy of in vitro KU-treated aNK cells was evaluated following adoptive transfer NK cell therapy in HCT models. We first

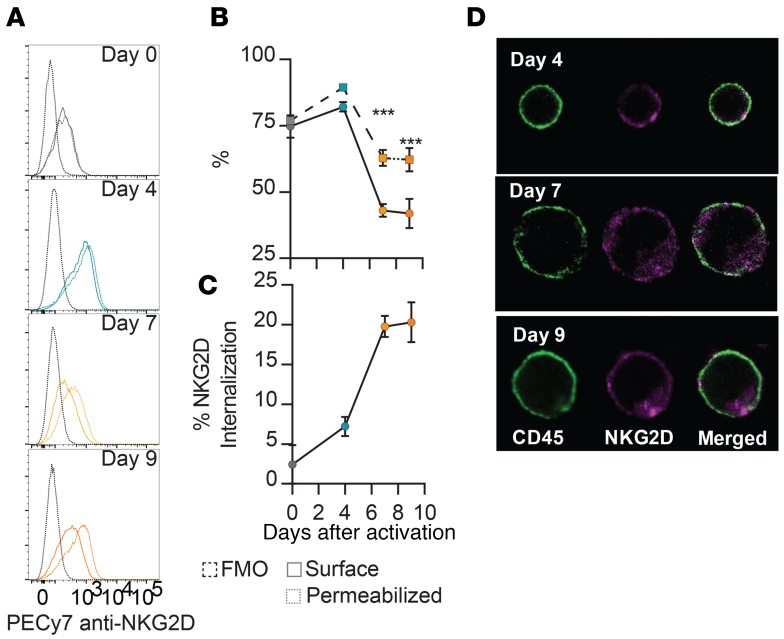

Figure 4. NKG2D internalization correlates with NCE after sustained in vitro stimulation. WT-derived NK cells were collected at different time points after in vitro IL-2 stimulation to represent the different stages of chronic stimulation. Thus, cells collected on day 0 represent the control unstimulated group (gray), on day 4 the acute group (turquoise), and on days 7 and 9 the chronic stimulation group (orange). (**A**) Representative histograms of the expression of NKG2D before (surface, straight line) and after cell permeabilization (dotted line), depicting the degree of protein internalization, are shown for gated NK cells. (**B** and **C**) The percentage of NKG2D before and after cell permeabilization (**B**) and the difference (NKG2D internalization) (**C**) on gated NK cells are shown. (**D**) Representative immunofluorescence image of NK cells expressing CD45 and NKG2D at days 4, 7, and 9 after stimulation. Data are representative of 3 independent experiments performed in triplicate (mean ± SEM). Two-way ANOVA was used to assess significance (***$P < 0.001$).

tested this therapy in an allogeneic HCT model of A20-tumor bearing BALB/c mice, given the expression of H60 by this B cell lymphoma tumor cell line that allows NKG2D-dependent killing and the success of NK cells in eliminating hematological cancers in HCT settings. Similar to previous reports, the freshly isolated NK (fresh NK), but not ex vivo IL-2 aNK, cell infusion resulted in superior tumor survival compared with untreated IL-2 control mice (Figure 6H and ref. 7). Administration of ex vivo activated KU-treated aNK cells resulted, however, in a significant increase in survival compared with untreated control mice ($P = 0.0007$) and mice receiving fresh NK cells ($P = 0.02$). When ex vivo KU-treated aNKs were infused into B16F10 tumor-bearing mice after syngeneic HCT, similar benefits on tumor survival were obtained, indicating that NKG2D-independent mechanisms are also improved by KU (Figure 6I). The augmented antitumor effects were the result of the effect of KU on NK cell function, as no differences in in vivo proliferation and survival capacities were observed between C57BL/6 L2G85 *luc*$^+$ control- and KU-treated aNK cells, where fresh NK cells showed the strongest response to IL-2 in BALB/c Rag2$^{-/-}$IL-2Rcγ$^{-/-}$ mice (Supplemental Figure 11). Additionally, the efficacy of KU treatment was only sustained during IL-2 administration, as cessation of stimulation resulted in the well-described NK cell contraction phenomenon in all groups due to cytokine dependency (Supplemental Figure 11). Overall, these data demonstrate that the inhibition of the ATM DNA damage repair pathway can improve in vivo antitumor responses of NK cell–adoptive therapy.

In summary, we have identified an exhaustion phenotype signature characterized by downregulation of activating receptors, such as NKG2D, and TFs, such as Eomes, while maintaining expression of KLRG1 (Figure 7A). This phenotype is accompanied by a reduction of NK cell proliferation as measured by Ki67 expression and of function regarding cytotoxicity and cytokine production. We suggest that this exhaustion is caused by the induction of DNA damage during acute activation that, by sustained stimulation, leads to downregulation of activating receptors, upregulation of the stress molecule MULT1, internalization of NKG2D, and reduction of NK cell function. Thus, inhibition of the activation of the DNA damage repair pathway can delay exhaustion and prolong NK cell proliferation, survival, and functionality and contribute to a promising therapeutic application in cancer therapy (Figure 7B).

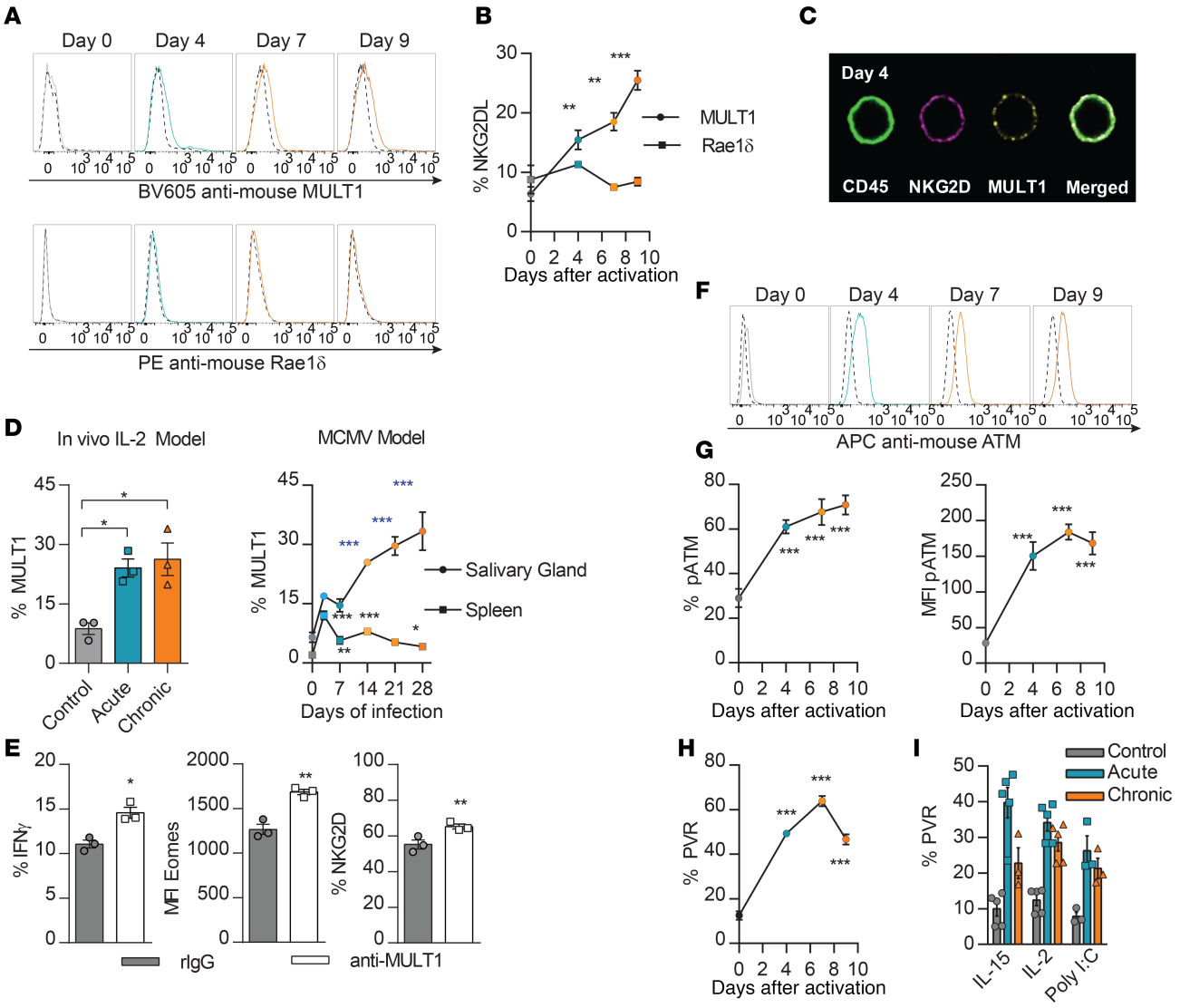

Figure 5. Expression of stress molecules and induction of DNA damage are increased during sustained NK cell stimulation. (**A** and **B**) Representative histograms (**A**) and total percentage (**B**) of MULT1 and Rae-1δ on gated NK cells are shown at different time points after in vitro IL-2 stimulation. (**C**) Representative immunofluorescence image of CD45, NKG2D, and MULT1 on NK cells on day 4 (acute stage) of in vitro IL-2 activation. (**D**) The total percentage of MULT1 on gated NK cells after in vivo IL-2 stimulation or in vivo MCMV infection is shown. (**E**) The total percentage of IFN-γ (after NK1.1 stimulation), Eomes MFI, and percentage of NKG2D are shown on gated NK cells collected after 9 days (chronic) in vitro IL-2 stimulation, which were treated with 10 μg/mL rIgG or anti-MULT1 5 days before. (**F** and **G**) Representative histograms (**F**) and the total percentage and MFI (**G**) of phosphorylated ATM (pATM) are shown for gated NK cells collected at different time points (control, day 0; acute, day 4; and chronic, days 7 and 9) after in vitro IL-2 stimulation. (**H** and **I**) The total percentage of PVR (CD155) is shown on gated NK cells after in vitro IL-2 stimulation (**H**) or after in vivo IL-15, IL-2, or Poly I:C stimulation (**I**). Data are representative of 3 (**A**–**D**, **F**, and **G**) or 2 (**E**) independent experiments. In vitro studies were done in triplicate, while in vivo studies were done with 3 mice per group, except for the MCMV model, which had 4–5 mice per group (mean ± SEM). Significant differences are displayed for comparisons with nonstimulated controls (*$P < 0.05$, **$P < 0.01$, ***$P < 0.001$).

Discussion

NK cells remain a promising cell population for adoptive immunotherapy; however, multiple mechanisms have been attributed to the lack of response of NK cell–based therapy against cancer, such as the presence of an immunosuppressive environment or NK cell–specific tumor evasion mechanisms (1). However, in recent years, the finding that NK and T cells undergo exhaustion following prolonged stimulation has proven to be an important biological process that regulates their function. Initially described upon tumor exposure, this study shows that NCE is induced following chronic stimulation with cytokines or infectious agents, suggesting that NK cell activation is a highly regulated phenomenon and that the induction of exhaustion might represent a self-regulatory mechanism that prevents exaggerated, overexuberant NK cell responses. We also identified

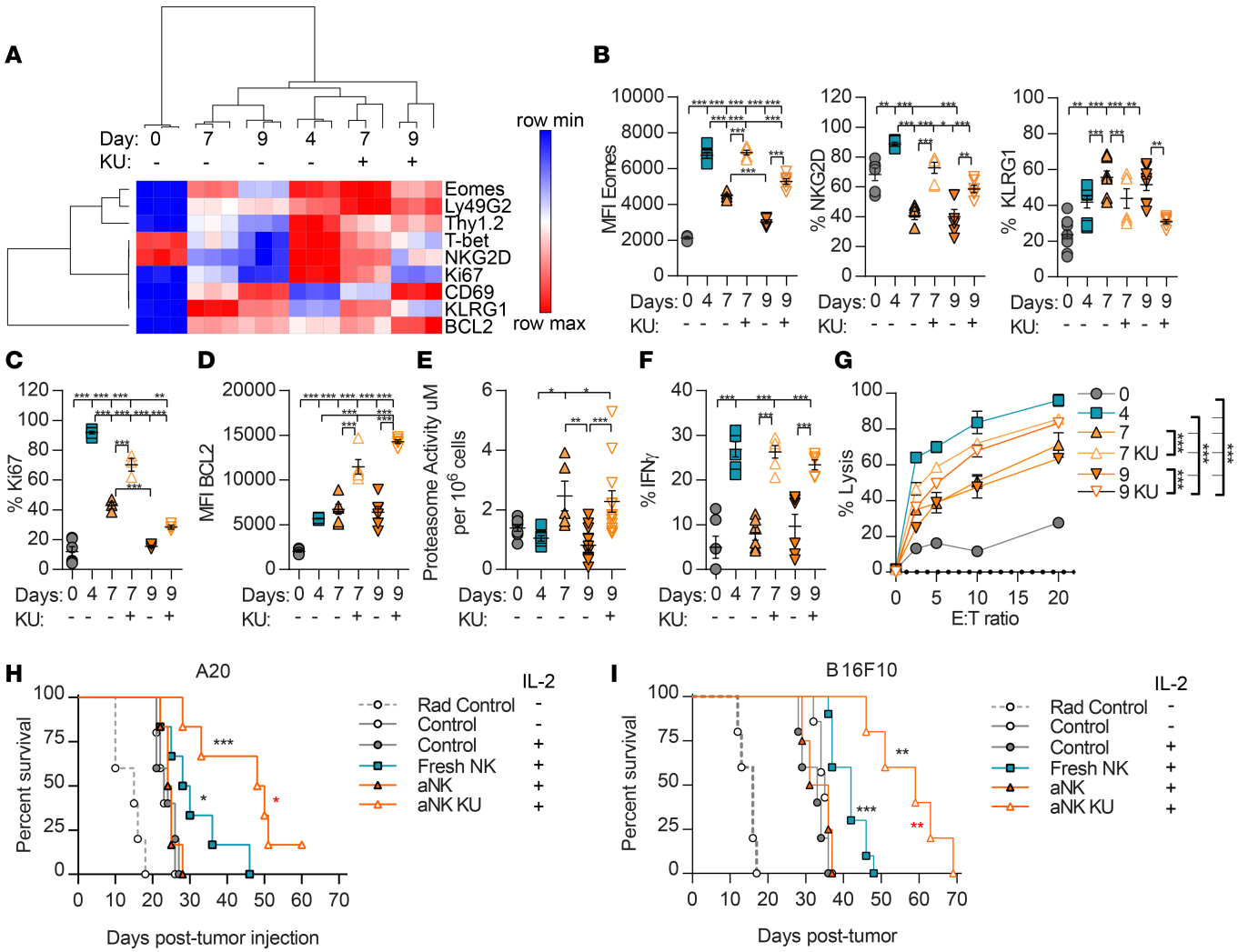

Figure 6. Inhibition of the ATM DNA damage repair pathway delays NCE by increasing NK cell function and survival, which improve antitumor responses after NK cell adoptive transfer therapy. Thy1.2 BM-derived cells were cultured in vitro with IL-2 and treated with DMSO or 7.5 μM ATM inhibitor KU on day 4 of culture. Adherent NK cells were collected at different time points of culture. (**A**) Hierarchical clustering by Euclidean distance analysis of the expression of multiple NK cell markers is shown. (**B**) The NCE phenotype was evaluated on in vitro activated NK cells measured by Eomes MFI and the total percentage of NKG2D and KLRG1 on gated NK cells. (**C**) The percentage of Ki67 is shown. (**D**) BCL2 MFI is shown on gated NK cells. (**E**) The 20S proteasome activity of NK cells is shown. (**F**) The percentage of IFN-γ production after NK1.1 stimulation is shown. (**G**) The percentage of tumor lysis of NK cells against A20 is shown. (**H** and **I**) C57BL/6 mice received total body radiation (TBI) at the time of tumor i.v. infusion (**H**: A20) or 7 days after tumor administration (**I**: B16F10), followed by allogeneic (**H**) or syngeneic (**I**) hematopoietic stem cell transplantation (HCT), along with freshly isolated unstimulated NK cells (fresh NK) or 5 day ex vivo expanded activated NK cells in the presence of vehicle control (aNK) or KU (KU aNK). When indicated, mice received low doses of IL-2 (5×10^4 IU) for 7 days after NK cell administration. Percentage is of in vivo tumor survival of NKG2D-dependent (**H**: A20) or -independent (**I**: B16F10) tumor-bearing mice after HCT with adoptive transfer of PBS (control) or NK cells. Data represent 2 or 3 independent experiments done in triplicate (in vitro model) or with 5–8 mice per group (in vivo tumor model) (mean ± SEM). One-way ANOVA (in vitro model) or log-rank test (in vivo tumor model) were used to assess significance (*$P < 0.05$, **$P < 0.01$, ***$P < 0.001$). In tumor models, the significance between control IL-2 and fresh NK and control IL-2 and KU-aNK (black asterisks) as well as between fresh NK and KU-aNK (red asterisks) is shown.

key proteins in NCE, highlighting the importance of the expression of Eomes, NKG2D, and KLRG1. These phenotypic markers of exhaustion could allow for the identification of exhaustion during NK cell–based cancer therapies to follow NK cell efficacy and potential antitumor response during the course of therapy.

High expressions of Eomes, T-bet, NKG2D, Ly49G2, and Thy1.2 have been frequently linked to an activation phenotype (4, 29), and downregulation of these markers during exhaustion suggests reduction of their activation status. In contrast, KLRG1 expression continues to increase during chronic stimulation. On NK cells, KLRG1 is acquired during cell differentiation and maturation, and its expression is significantly increased during cell activation and homeostatic proliferation (30). However, higher expression of KLRG1 has been previously described during MCMV infection, sustained IL-15 treatment, or tumor exposure and

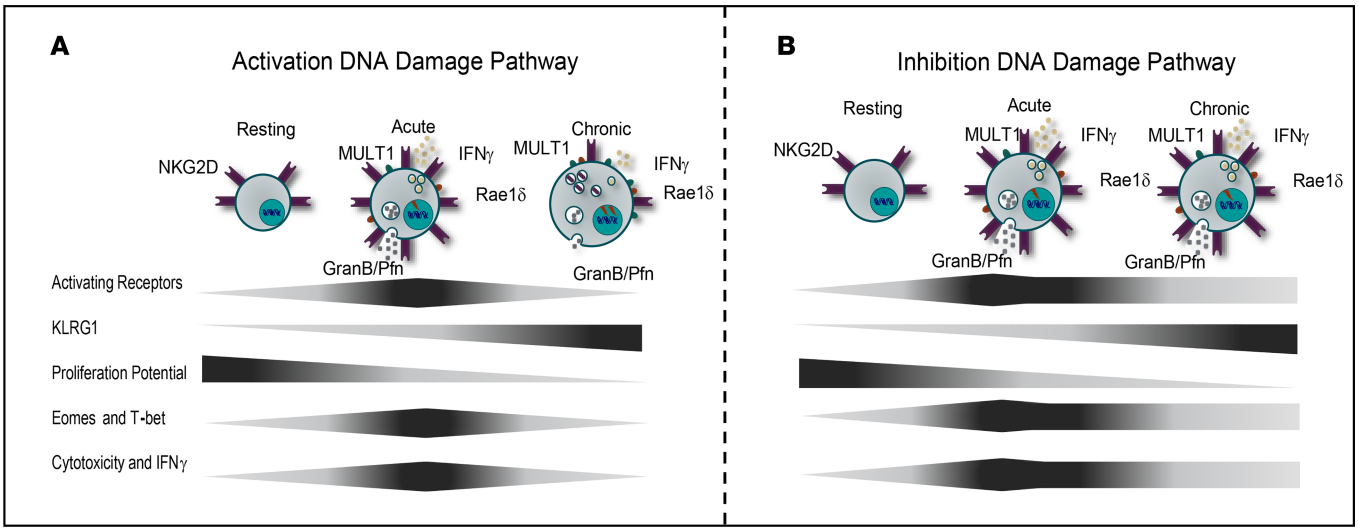

Figure 7. Schematic representation of the implication of the DNA damage repair pathway in NCE. (**A**) During acute stimulation, NK cells present the highest expression of activating receptors, proliferation potential, activating transcription factors, and functionality. This process leads to the activation of the DNA damage repair pathway that, with continued stimulation, leads to upregulation of stress molecules, such as MULT1; internalization of NKG2D; and reduction of proliferation, function, and expression of activating receptors and transcription factors. (**B**) Inhibition of this pathway by KU during the acute phase can delay the exhaustion phenotype and prolong NK cell function, proliferation, and the activation phenotype.

also has been connected to decreased NK cell function (7, 12, 30). These studies and our results suggest that, similar to the early activating role assigned to the inhibitory receptor Ly49G2 (4, 29), KLRG1 seems to behave as an activation marker during the peak of NK cell activation but additionally as an early senescence marker after chronic stimulation of NK cells, similar to T cells (20).

We have demonstrated that NKG2D is involved in the induction of NCE, as the absence or blockade of NKG2D can delay the development of exhaustion during chronic stimulation, resulting in preserved biological function. This result might be seen as contradictory to the common view of NKG2D function. The NKG2D receptor plays an important role in NK cell physiology by regulating NK cell development, homeostasis, and survival (31). Additionally, NKG2D is also involved in graft rejection (32), autoimmunity (33–35), infection (36), and, more importantly, during immunosurveillance, as it has proven to be critical in both NK and T cell antitumor responses (37). Indeed, NKG2D behaves as a molecular sensor that recognizes and eliminates stress-affected cells through the binding to stress molecules (31, 37). However, and in accordance with our results, an upregulation of IFN-γ and resistance to MCMV infection have been observed in NKG2D$^{-/-}$ mice (31, 38). Similarly, NKG2D-deficient mice were capable of better controlling tumor growth and survival of melanoma tumor-bearing mice because of a stronger response to stimuli, particularly through NKp46 (38, 39). This improvement of NK cell function by NKG2D-KO mice has been recently correlated with a role of NKG2D during NK cell development that influences NKp46 activation threshold by negatively regulating NKp46 signaling (38). This phenomenon could also be a contributing factor on NCE. The fact that a similar effect is observed during acute blockade of NKG2D by mAb therapy further supports the concept that NKG2D plays a significant role in NCE. A role of NKG2D in NK cell desensitization has also been suggested due to the ability of NKG2D-deficient NK cells to respond to a higher extent not only to NKp46, but also to NK1.1- and CD16-stimulated NK cells, which more highly correlates with what we see (38, 39).

Additionally, recent studies have also suggested a role of NKG2D in NK cell survival (31, 40). Poggi and colleagues demonstrated that the binding between NKG2D and tumor-expressing NKG2DLs causes apoptosis of human NK cells (40). Similarly, cell death resulted after cocultures between mouse NK cells and Rae-1–expressing tumor cells in an NKG2D-dependent manner (41). Our results are in agreement with these studies, as prevention of binding between NKG2D and MULT1 diminished the NCE phenotype both in vivo and in vitro. Thus, our data indicate that NCE could represent a necessary stage prior to cell death of chronically stimulated and highly aNK cells. However, other alternatives are possible, as Madera and colleagues reported NK cell fratricide due to upregulation of NKG2DL on NK cells after exposure to MCMV infection (42).

The reduction of NKG2D expression and, consequently impaired NK cell function, was initially described after exposure to NKG2DL-expressing tumor cells, when soluble forms of NKG2DL or TGF-β were released by tumor cells (43). Interestingly, high levels of NKG2DL have been previously described not only on transformed cells (26), but also on immune cells exposed to a variety of stimulatory molecules, such as alloreactive T cells, and after bacterial or viral infection (44), preventing graft-versus-host disease and pathological damage, respectively. Rae-1ε, for example, has been found to be constitutively expressed on lymph node endothelial cells, but its expression is highly induced on tumor-associated endothelial cells (35). The upregulation of NKG2DL has also been linked to NK cell fratricide during MCMV infection (42). MCMV also led to upregulation of Rae-1 on fibroblasts (45) and DCs (46), affecting NKG2D expression and NK cell function. NKG2D importance during MCMV is demonstrated by the fact that immune evasion through proteins encoded by m145, m152, and m155 modulate the expression of MULT1, Rae-1, and H60, respectively, on infected cells (47, 48). Interestingly, in our study, NKG2D downregulation was associated with the induction of NKG2D internalization and was correlated to increased levels of expression of MULT1 on NK cells during chronic stimulation. Downregulation of NKG2D has also been reported in MULT1-expressing B16 tumor cells (39), whereas such downregulation was not observed in B16 tumors capable of secreting soluble MULT1, suggesting a role for endogenous NKG2DL interaction in NK cell tumor desensitization (49). Similarly, NKG2D internalization was also involved upon endogenous Rae-1ε engagement, causing impaired NK cell function so that Rae-1–deficient mice displayed higher NKG2D MFI expression on B16 intratumor NK cells (39). Our study is the first to our knowledge to demonstrate an upregulation of MULT1 on NK cells during activation.

Within the murine NKG2DL family, MULT1 has the strongest binding affinity to NKG2D (50), and its expression is regulated by poly-ubiquitination of its cytoplasmic tail, revealing a proteasome-dependent degradation mechanism (51). In fact, proteasome inhibition by bortezomib increases the level of expression of ULBP1, the human equivalent of MULT1 (52). Similarly, proteasome activity was reduced after sustained stimulation in our model and was correlated to MULT1 expression accumulation. Furthermore, downregulation of the proteasome activity negatively affects BCL2 expression due to accumulation of proapoptotic proteins (Bax, Bid, Bim, etc.), and to prevention of nuclear translocation of the TF NF-κB (40), explaining a role of the proteasome in NK cell regulation of governing MULT1 and BCL2, and thus regulating survival.

The upregulation of stress molecules has been associated with both genotoxic and cellular stresses, such as chemotherapy, dysregulated proliferation, and oxidative stress, which result in the activation of the DNA damage repair pathways by phosphorylation of ATM. ATM behaves as a DNA damage sensor capable of orchestrating a cellular response (26, 51, 53) and can also regulate the phosphorylation of the histone H2AX (γH2AX), a sensor for DNA double-strand breaks (ref. 54). It was reported that inhibition of ATM prevents the expression of stress molecules on tumor cells (26), aphidicolin-treated fibroblasts (26), and antigen-activated T cells (53). Our data demonstrated that sustained stimulation results in DNA damage and consequent activation of the ATM DNA response and repair pathways. In agreement with our results, higher levels of γH2AX were also detected in hyperresponsive NK cells from immunodeficient mice (54). Furthermore, and similar to our study, the repetitive exposure of human NK cells to IL-15 in vitro, also caused NCE with a reduction in proliferation, survival, and function of human NK cells, as we similarly observed in our murine model. In this study, the effect on sustained exposure to IL-15 was also independent of changes in the expression of CD122 and CD132 (18). Felices and coworkers showed that these exhausted human NK cells have an enrichment of genes involved in cell cycle checkpoint and cell cycle arrest that correlate with an increase in cellular damage and stress due to failure to properly repair the DNA damage, likely directing the activation of programmed cell death pathways (18). Taking these studies into consideration, it follows that the blockade of the DNA damage repair pathway with KU results in a higher survival, a more sustained activating phenotype and superior functional capacities of NK cells. These data therefore provide evidence of the mechanisms responsible for controlling NK cell activation and exhaustion during sustained stimulation. Our study suggests that, due to continued proliferation during chronic stimulation, there is DNA damage, which triggers the activation of the ATM DNA damage pathway and causes exhaustion. Our data also indicate that activation of this pathway is responsible for the expression of stress molecules contributing to NKG2D internalization and impaired expression of activating and inhibitory receptors and, more importantly, for limiting NK cell functional capacities.

A previous study demonstrated that overexpression of IL-15 caused chromosomal instability and DNA hypermethylation on large granular lymphocyte leukemia cells mediated by induction of Myc/NF-κp65/Hdac-1 that results in overexpression of the DNA methyltransferase Dnmt3b (55). Although we cannot

completely exclude this mechanism in the induction of NCE, we did not observe any difference in the mRNA expression of Dnmt3b during in vitro stimulation of NK cells. However, an upregulation of the mRNA of Dnmt1, another DNA methyltransferase, at the peak of stimulation was observed, which might suggest an activation of the DNA damage response in a DNA methylation-independent manner (55).

Unlike previous studies (6, 10, 11, 16, 56), Tim3 and PD1 were not involved in NCE in our models. Indeed, Tallerico and colleagues observed an upregulation of Tim-3 and PD-1 after sustained exposure to IL-15 on human NK cells and that the expression of these markers along with the presence of high levels of IL-15 in the serum could predict the response toward anti-CTLA4 therapy in melanoma patients (56). However, in our in vitro model Tim3 blockade did not restore function (data not shown), and PD1 expression was not meaningfully detected in any of our models expect for the MCMV models. The fact that we used murine models could account for these disparities. Thus, given the role of PD-L1/PD1 in the regulation of apoptosis, anergy, and exhaustion, we cannot totally reject the possibility that PD1 is indirectly involved in NCE, and, therefore, further analysis is needed. The cytokine-inducible SH2-containing protein (CIS) is another checkpoint inhibitor for which expression has been shown to limit the IL-15 response, as NK cells from *Cish*$^{-/-}$ mice display superior functional capacities (57). In our study, however, we did not observe differences in the expression of mRNA *Cish* between control- and KU-treated NK cells after chronic in vitro IL-2 stimulation.

This study has substantial clinical ramifications; currently many NK cell–based therapies rely on robust and continued stimulation to achieve stronger functional approaches that may cause NCE. Therefore, the analysis of NCE during the course of activation and treatment will be necessary to predict the antitumor response of NK cells. Additionally, the development of strategies that inhibit or delay NCE could significantly improve NK cell–based therapies of cancer. Here, we have demonstrated that the treatment of ex vivo aNK cells with KU was successful in maintaining NK cell activation and in achieving markedly improved antitumor responses. These data, therefore, support the ATM DNA damage pathway as a putative candidate to target exhaustion on NK cells and improve antitumor responses in NK cell adoptive therapies.

Methods

Additional details can be found in Supplemental Methods.

Mice

WT C57BL/6 (H-2^b) and BALB/c (H-2^d) mice were purchased from The Jackson Laboratory. C57BL/6 KLRK1$^{-/-}$ (NKG2D$^{-/-}$) mice were a gift from David Raulet (University of California, Berkeley, Berkeley, California, USA) and bred in our animal facility. Female mice were used at 8–12 weeks of age and housed under specific pathogen–free conditions.

Cell lines

The A20 leukemia tumor cell line, the B16F10 melanoma tumor cell line, and the Yac1 cell line were purchased from ATCC. Cells were growth in RPMI 1640 media supplemented with 10% heat-inactivated FBS, 1 mmol/L sodium pyruvate, 2 mmol/L glutamine, 0.1 mmol/L nonessential amino acids, 100 U/mL penicillin, and 100 μg/mL streptomycin at 37°C with 5% CO_2. Cells were collected for tumor or in vitro studies when they reach exponential growth during the week of culture. The cells were tested for mycoplasma negativity according manufacture's instructions using the universal mycoplasma detection kit (ATCC).

In vivo NK cell stimulation model

Mice were treated with known NK cell activation reagents in order to chronically stimulate NK cells (Supplemental Figure 6). A detailed description of the reagents and regimens used for each model can be found below.

Chronic IL-15 stimulation model. C57BL/6 mice were treated i.p. with 2.5 μg recombinant human IL-15 (NCI Repository, Frederick, Maryland, USA) and 3 μg recombinant mouse IL-15Rα human IgG1 fusion chimera protein (R&D Systems, 551-MR) as previously described (12) (Supplemental Figure 1A). Briefly, mice were treated 14 and 12 days (resolved group); 14, 12, 9, 7, 5, and 2 days (chronic group); or 2 days (acute group) prior to organ collection. Control groups received PBS instead of IL-15/ IL-15Rα.

Chronic IL-2 stimulation model. C57BL/6 or NKG2D$^{-/-}$ (KO) mice were treated with PBS (control group) or 5×10^5 IU recombinant human IL-2 (NCI Repository) 10 and 9 days (resolved group); 10, 9, 6, 5, 2, and 1 days (chronic group); or 2 and 1 days (acute group) prior to organ collection (Supplemental Figure 1B).

For NKG2D blocking experiments, mice received 200 μg anti-NKG2D (clone C7) or control γ globulin (IgG) 2 days prior to IL-2 treatment and again 4 days later.

Chronic TLR3 stimulation model. Following the same schedule described for the IL-2 model, C57BL/6 mice were treated with 200 μg Poly I:C (MilliporeSigma, P1530) to indirectly induce NK activation through induction of IL-12, IL-18 and type I IFN production. PBS was used as control (Supplemental Figure 1B).

Chronic MCMV stimulation model. C57BL/6 mice were injected with 2.5×10^4 plaque forming units of MCMV i.p. 3, 7, 14, 21, or 28 days before organ collection. Control mice received RPMI. The MCMV Smith strain was provided in-house and maintained by propogation in salivary glands in 6-week-old BALB/c mice as previously described (58). Salivary glands were processed as previously described (23).

In vitro NK cell stimulation model

Single-cell suspensions from BM and spleens of mice were T cell–depleted using the CD90 positive selection kit (StemCell Technology) according to manufacturer's instructions and cultured in RPMI complete media at 37°C with 5% CO_2 and with 10^3 IU/mL IL-2. In some experiments, NKG2D-KO or WT mice were used. At day 4, cells were treated with 7.5 μM KU (Calbiochem EMD Millipore), 20 μg/mL anti-MULT1 (R&D Systems), or controls when indicated. Activated lymphocyte adherent killer cells, which represent 90% of purified NK cells (59), were collected at multiple time points (day 0, control; day 4, acute; days 7 and 9, chronic) to analyze NK cell activation and function.

Analysis of NK cell phenotype

Antibody staining of single-cell suspensions was performed as previously described (60). For TFs, the Foxp3/TF staining buffer kit (Ebioscience) was used according to the manufacturer's instructions. See Supplemental Table 1 for detailed description of antibodies used in this study.

DNA damage repair pathway. To evaluate phosphorylation of ATM and Chk2, after cell surface staining with anti-NK1.1 and anti-TCRβ, cells were fixed with 4% formaldehyde for 10 minutes at room temperature, followed by permeabilization with –20°C methanol for 30 minutes on ice. Cells were then incubated for 30 minutes at 4°C with normal rabbit IgG (Cell Signaling Technology) and followed by a 1-hour staining with antibody directed to the phosphorylated Alexa Fluor 647 (AF647) ATM, purified Chk2, or isotype control. For Chk2, cells were then stained for 10 minutes at 4°C with AF647 goat anti-rabbit (Invitrogen).

NKG2D internalization by flow cytometry. Anti-NKG2D or rat IgG1 was utilized on in vitro expanded NK cells before and/or after permeabilization using the Foxp3/TF staining buffer kit according to the manufacturer's instructions. The difference between the percentage of cell surface expression of NKG2D before and after permeabilization represent the percentage of internalization.

NKG2D internalization by immunofluorescence. Cells were incubated with goat serum to prevent nonspecific binding for 1 hour at 4°C and then incubated for 3 hours at 4°C with anti-CD45 mAb (AF488). Cells were fixed with 4% formaldehyde for 10 minutes at room temperature in a Lab-tek II chamber slide (Thermo Fisher Scientific). Cells were then incubated with purified anti-NKG2D (Santa Cruz Biotechnology) or isotype control diluted in an antibody dilution buffer (ADB) that contained 3% FBS and 0.2% saponin in 1× PBS overnight. Secondary staining with anti-mouse IgM (AF647) was performed in ADB for 3 hours at 4°C. Finally, cells were air dried and slides were mounted with DAPI mounting media (Vector Laboratories Inc.). NK cells were visualized using a LSM 880 inverted confocal microscope (Carl Zeiss). Images were analyzed using ZEN 2.3 lite blue edition (Carl Zeiss).

MULT1 and NKG2D detection by immunofluorescence. Cells were first incubated with goat serum to prevent nonspecific binding for 1 hour at 4°C. Cells were incubated overnight at 4°C with anti-CD45 (AF488), anti-NKG2D, and anti-MULT1. Secondary staining with anti-mouse IgM (AF647) and anti-Armenian Hamster IgG1 biotin was performed for 3 hours at 4°C, followed by Streptavidin (AF594) (Thermo Fisher Scientific). NK cells were visualized using LSM 880 inverted confocal microscope (Carl Zeiss). Images were analyzed using ZEN 2.3 lite blue edition (Carl Zeiss).

Analysis of NK cell function

CFSE-based cell killing assay. Splenocytes, adherent NK cells, or freshly isolated NK (fresh NK) cells using an NK cell negative selection kit (StemCell Technology) were cultured at multiple effector/target (E/T) ratios with CFSE-labeled Yac-1 or A20 tumor cells (ATCC) for 4 hours and analyzed by flow cytometry. All techniques were performed according to the manufacturer's instructions, and the percentage of lysis

was calculated as previously described (4). When splenocytes were used, the E/T ratio was normalized to the proportion of NK cells present among the splenocytes.

IFN-γ production. Splenoctyes, adherent NK cells, or freshly isolated NK cells were stimulated for 4 hours with 10 μg/mL plate-bound anti-NK1.1 (PK136) or mIgG2a for CD16 stimulation as previously described (60, 61).

Data analysis

Multivariate heatmap. Flow cytometry data obtained from in vivo chronic stimulation models were represented in a multivariate heatmap utilizing the ggplot package in Rstudio (version 1.0.153, RStudio Inc.) and R version 3.2.0. For MFI, data were normalized by calculating the MFI average for each marker and dividing each value by this average, so the maximal and minimal expression of each marker for each model could be visualized.

PCA. PCA analysis was performed using the RStudio ggfortify package on the values obtained by flow cytometry. The two dominant principal components were plotted against one another to assess the relationships between the different treatments, and the PCA loading vectors (eigenvectors) were also represented.

Microarray Analysis. Detailed description of microarray analysis can be found in the Supplementary Methods. The microarray data discussed in this publication have been deposited in NCBI's Gene Expression Omnibus and are accessible through GEO Series accession number GSE131522.

Hierarchical clustering. Hierarchical clustering analysis using Euclidean distance was performed with the values obtained by flow cytometry of the in vitro model (MFI for Eomes, Ly49G2, Thy1.2, and BCL2 or percentage for NKG2D, T-bet, Ki67, CD69, and KLRG1) using Morpheus (Broad Institute, Cambridge, Massachusetts, USA). Each row represents the maximal and minimal expression for any given marker.

Tumor models

NKG2D-dependent tumor model. BALB/c mice were lethally irradiated (825 cGy) 2 days before i.v. injection of 5×10^6 NK- and T cell–depleted C57BL/6 bone marrow cells along with 10^5 B cell lymphoma A20 cells to minimize the effect of radio-resistant host-type NK cells. Some mice also received 10^6 freshly isolated C57BL/6-derived NK cells (fNK), isolated according to the manufacturer's instructions (StemCell Technology), or ex vivo IL-2–expanded aNK cells. Ex vivo aNK cells were treated with DMSO vehicle control (aNK) or 7.5 μM ATR/ATR kinase inhibitor KU (aNK KU) on day 3 of culture, and adherent NK cells were collected 2 days later.

NKG2D-independent tumor model. Mice were injected i.v. with 2×10^5 cells of the B16F10 metastatic melanoma tumor cell line. After 7 days, mice underwent syngeneic HCT. Briefly, C57BL/6 mice underwent lethal irradiation (950 cGy) and were injected i.v. with 5×10^6 C57BL/6 bone marrow cells. As in the previous model, mice received fNK, aNK, or aNK KU. In both models, mice received daily i.p. injections of 5×10^4 IU IL-2 for 7 days where indicated and were monitored for survival and euthanized when moribund.

Statistical analysis

Each experiment was performed at least 2 times with 3–5 mice per group. Student's 2-tailed *t* test, 1-way ANOVA (Bonferroni post test analysis), 2-way ANOVA (Bonferroni post test analysis), and log-rank test were used when appropriate to determine statistical significance (Graphpad Prism 4). *P* values were considered statistically significant at $P < 0.05$.

Study approval All animal protocols were approved by the IACUC at Stanford University.

Author contributions

MA designed and performed research, analyzed data, and wrote the manuscript. FS, JB, ASW, and ARM conducted experiments. WJM provided essential reagents. FS, AP, and WJM provided scientific input and assisted with the preparation of the manuscript. RSN provided overall scientific guidance and helped to write the manuscript.

Acknowledgments

This work was supported by National Institute of Health grants R01CA125276 and P01CA049605 and the Skippy Frank Foundation. MA was supported by the American Association for Cancer Research–Millennium Fellowship in Lymphoma Research (15-40-38-ALVA). FS was supported by the Geneva University Hospitals, the Swiss Cancer League, the Fondation Genevoise de bienfaisance Valeria Rossi di Montelera,

and the Dubois-Ferrière-Dinu-Lipatti Foundation. We thank the Stanford Protein and Nucleic Acid core facility; the Stanford shared FACS facility; and Sara Clark, Paul Richardson, and Jose Antonio Seonae Fernandez for their technical assistance. We also thank David Raulet for providing the NKG2D-deficient mice and the NCI repository for providing the IL-2 and IL-15. Finally, we wish to thank all the members of RSN's laboratory for the valuable help and discussion through the course of this project.

Address correspondence to: Maite Alvarez, Center for Clinical Sciences Research Building, Room 2210, 269 West Campus Drive, Stanford, California 94305, USA. Phone: 650.723.9655; Email: malv015@stanford.edu. Or to: Robert S. Negrin, Center for Clinical Sciences Research Building, Room 2205, 269 West Campus Drive, Stanford, California 94305, USA. Phone: 650.723.0822; Email: negrs@stanford.edu.

1. Wahid SF. Indications and outcomes of reduced-toxicity hematopoietic stem cell transplantation in adult patients with hematological malignancies. *Int J Hematol*. 2013;97(5):581–598.
2. Simonetta F, Alvarez M, Negrin RS. Natural killer cells in graft-versus-host-disease after allogeneic hematopoietic cell transplantation. *Front Immunol*. 2017;8:465.
3. Mamessier E, et al. Human breast cancer cells enhance self tolerance by promoting evasion from NK cell antitumor immunity. *J Clin Invest*. 2011;121(9):3609–3622.
4. Alvarez M, Bouchlaka MN, Sckisel GD, Sungur CM, Chen M, Murphy WJ. Increased antitumor effects using IL-2 with anti-TGF-β reveals competition between mouse NK and CD8 T cells. *J Immunol*. 2014;193(4):1709–1716.
5. Buyse M, et al. Individual patient data meta-analysis of randomized trials evaluating IL-2 monotherapy as remission maintenance therapy in acute myeloid leukemia. *Blood*. 2011;117(26):7007–7013.
6. Gallois A, Silva I, Osman I, Bhardwaj N. Reversal of natural killer cell exhaustion by TIM-3 blockade. *Oncoimmunology*. 2014;3(12):e946365.
7. Gill S, et al. Rapid development of exhaustion and down-regulation of eomesodermin limit the antitumor activity of adoptively transferred murine natural killer cells. *Blood*. 2012;119(24):5758–5768.
8. Simonetta F, Pradier A, Roosnek E. T-bet and Eomesodermin in NK Cell Development, Maturation, and Function. *Front Immunol*. 2016;7:241.
9. Shehata HM, Hoebe K, Chougnet CA. The aged nonhematopoietic environment impairs natural killer cell maturation and function. *Aging Cell*. 2015;14(2):191–199.
10. Beldi-Ferchiou A, et al. PD-1 mediates functional exhaustion of activated NK cells in patients with Kaposi sarcoma. *Oncotarget*. 2016;7(45):72961–72977.
11. Norris S, Coleman A, Kuri-Cervantes L, Bower M, Nelson M, Goodier MR. PD-1 expression on natural killer cells and CD8(+) T cells during chronic HIV-1 infection. *Viral Immunol*. 2012;25(4):329–332.
12. Elpek KG, Rubinstein MP, Bellemare-Pelletier A, Goldrath AW, Turley SJ. Mature natural killer cells with phenotypic and functional alterations accumulate upon sustained stimulation with IL-15/IL-15Ralpha complexes. *Proc Natl Acad Sci USA*. 2010;107(50):21647–21652.
13. Huergo-Zapico L, et al. Expansion of NK cells and reduction of NKG2D expression in chronic lymphocytic leukemia. Correlation with progressive disease. *PLoS ONE*. 2014;9(10):e108326.
14. Parry HM, et al. NK cell function is markedly impaired in patients with chronic lymphocytic leukaemia but is preserved in patients with small lymphocytic lymphoma. *Oncotarget*. 2016;7(42):68513–68526.
15. Coudert JD, et al. Altered NKG2D function in NK cells induced by chronic exposure to NKG2D ligand-expressing tumor cells. *Blood*. 2005;106(5):1711–1717.
16. Seo H, et al. IL-21-mediated reversal of NK cell exhaustion facilitates anti-tumour immunity in MHC class I-deficient tumours. *Nat Commun*. 2017;8:15776.
17. Simonetta F, Pradier A, Bosshard C, Masouridi-Levrat S, Chalandon Y, Roosnek E. NK Cell Functional Impairment after Allogeneic Hematopoietic Stem Cell Transplantation Is Associated with Reduced Levels of T-bet and Eomesodermin. *J Immunol*. 2015;195(10):4712–4720.
18. Felices M, et al. Continuous treatment with IL-15 exhausts human NK cells via a metabolic defect. *JCI Insight*. 2018;3(3):e96219.
19. Wang JM, et al. KLRG1 negatively regulates natural killer cell functions through the Akt pathway in individuals with chronic hepatitis C virus infection. *J Virol*. 2013;87(21):11626–11636.
20. Crespo J, Sun H, Welling TH, Tian Z, Zou W. T cell anergy, exhaustion, senescence, and stemness in the tumor microenvironment. *Curr Opin Immunol*. 2013;25(2):214–221.
21. Sun K, et al. Mouse NK cell-mediated rejection of bone marrow allografts exhibits patterns consistent with Ly49 subset licensing. *Blood*. 2012;119(6):1590–1598.
22. Kamimura Y, Lanier LL. Rapid and sequential quantitation of salivary gland-associated mouse cytomegalovirus in oral lavage. *J Virol Methods*. 2014;205:53–56.
23. Cortez VS, Fuchs A, Cella M, Gilfillan S, Colonna M. Cutting edge: Salivary gland NK cells develop independently of Nfil3 in steady-state. *J Immunol*. 2014;192(10):4487–4491.
24. Robbins SH, Tessmer MS, Mikayama T, Brossay L. Expansion and contraction of the NK cell compartment in response to murine cytomegalovirus infection. *J Immunol*. 2004;173(1):259–266.
25. Tessmer MS, Reilly EC, Brossay L. Salivary gland NK cells are phenotypically and functionally unique. *PLoS Pathog*. 2011;7(1):e1001254.
26. Gasser S, Orsulic S, Brown EJ, Raulet DH. The DNA damage pathway regulates innate immune system ligands of the NKG2D receptor. *Nature*. 2005;436(7054):1186–1190.

27. Cerboni C, Zingoni A, Cippitelli M, Piccoli M, Frati L, Santoni A. Antigen-activated human T lymphocytes express cell-surface NKG2D ligands via an ATM/ATR-dependent mechanism and become susceptible to autologous NK- cell lysis. *Blood*. 2007;110(2):606–615.
28. Müller AM, et al. Donor hematopoiesis in mice following total lymphoid irradiation requires host T-regulatory cells for durable engraftment. *Blood*. 2014;123(18):2882–2892.
29. Barao I, et al. Mouse Ly49G2+ NK cells dominate early responses during both immune reconstitution and activation independently of MHC. *Blood*. 2011;117(26):7032–7041.
30. Huntington ND, et al. NK cell maturation and peripheral homeostasis is associated with KLRG1 up-regulation. *J Immunol*. 2007;178(8):4764–4770.
31. Zafirova B, et al. Altered NK cell development and enhanced NK cell-mediated resistance to mouse cytomegalovirus in NKG2D-deficient mice. *Immunity*. 2009;31(2):270–282.
32. Ogasawara K, Benjamin J, Takaki R, Phillips JH, Lanier LL. Function of NKG2D in natural killer cell-mediated rejection of mouse bone marrow grafts. *Nat Immunol*. 2005;6(9):938–945.
33. Ogasawara K, et al. NKG2D blockade prevents autoimmune diabetes in NOD mice. *Immunity*. 2004;20(6):757–767.
34. Guerra N, et al. A selective role of NKG2D in inflammatory and autoimmune diseases. *Clin Immunol*. 2013;149(3):432–439.
35. Markiewicz MA, et al. RAE1ε ligand expressed on pancreatic islets recruits NKG2D receptor-expressing cytotoxic T cells independent of T cell receptor recognition. *Immunity*. 2012;36(1):132–141.
36. Huang M, Sun R, Wei H, Tian Z. Simultaneous knockdown of multiple ligands of innate receptor NKG2D prevents natural killer cell-mediated fulminant hepatitis in mice. *Hepatology*. 2013;57(1):277–288.
37. Guerra N, et al. NKG2D-deficient mice are defective in tumor surveillance in models of spontaneous malignancy. *Immunity*. 2008;28(4):571–580.
38. Jelencic V, et al. NK cell receptor NKG2D sets activation threshold for the NCR1 receptor early in NK cell development. *Nat Immunol*. 2018;19(10):1083–1092.
39. Thompson TW, et al. Endothelial cells express NKG2D ligands and desensitize antitumor NK responses. *Elife*. 2017;6:null.
40. Poggi A, Zancolli M, Boero S, Catellani S, Musso A, Zocchi MR. Differential survival of γδT cells, αβT cells and NK cells upon engagement of NKG2D by NKG2DL-expressing leukemic cells. *Int J Cancer*. 2011;129(2):387–396.
41. Nakamura K, et al. Fratricide of natural killer cells dressed with tumor-derived NKG2D ligand. *Proc Natl Acad Sci USA*. 2013;110(23):9421–9426.
42. Madera S, Rapp M, Firth MA, Beilke JN, Lanier LL, Sun JC. Type I IFN promotes NK cell expansion during viral infection by protecting NK cells against fratricide. *J Exp Med*. 2016;213(2):225–233.
43. Oppenheim DE, et al. Sustained localized expression of ligand for the activating NKG2D receptor impairs natural cytotoxicity in vivo and reduces tumor immunosurveillance. *Nat Immunol*. 2005;6(9):928–937.
44. Waggoner SN, Cornberg M, Selin LK, Welsh RM. Natural killer cells act as rheostats modulating antiviral T cells. *Nature*. 2011;481(7381):394–398.
45. Tokuyama M, Lorin C, Delebecque F, Jung H, Raulet DH, Coscoy L. Expression of the RAE-1 family of stimulatory NK-cell ligands requires activation of the PI3K pathway during viral infection and transformation. *PLoS Pathog*. 2011;7(9):e1002265.
46. Morvan MG, Champsaur M, Reizis B, Lanier LL. Chronic In Vivo Interaction of Dendritic Cells Expressing the Ligand Rae-1ε with NK Cells Impacts NKG2D Expression and Function. *Immunohorizons*. 2017;1(3):10–19.
47. Krmpotic A, et al. NK cell activation through the NKG2D ligand MULT-1 is selectively prevented by the glycoprotein encoded by mouse cytomegalovirus gene m145. *J Exp Med*. 2005;201(2):211–220.
48. Wang R, et al. Structural basis of mouse cytomegalovirus m152/gp40 interaction with RAE1γ reveals a paradigm for MHC/MHC interaction in immune evasion. *Proc Natl Acad Sci USA*. 2012;109(51):E3578–E3587.
49. Deng W, et al. Antitumor immunity. A shed NKG2D ligand that promotes natural killer cell activation and tumor rejection. *Science*. 2015;348(6230):136–139.
50. Carayannopoulos LN, Naidenko OV, Fremont DH, Yokoyama WM. Cutting edge: murine UL16-binding protein-like transcript 1: a newly described transcript encoding a high-affinity ligand for murine NKG2D. *J Immunol*. 2002;169(8):4079–4083.
51. Nice TJ, Coscoy L, Raulet DH. Posttranslational regulation of the NKG2D ligand Mult1 in response to cell stress. *J Exp Med*. 2009;206(2):287–298.
52. Butler JE, Moore MB, Presnell SR, Chan HW, Chalupny NJ, Lutz CT. Proteasome regulation of ULBP1 transcription. *J Immunol*. 2009;182(10):6600–6609.
53. Ardolino M, et al. DNAM-1 ligand expression on Ag-stimulated T lymphocytes is mediated by ROS-dependent activation of DNA-damage response: relevance for NK-T cell interaction. *Blood*. 2011;117(18):4778–4786.
54. Nishikii H, et al. DR3 signaling modulates the function of Foxp3+ regulatory T cells and the severity of acute graft-versus-host disease. *Blood*. 2016;128(24):2846–2858.
55. Mishra A, et al. Aberrant overexpression of IL-15 initiates large granular lymphocyte leukemia through chromosomal instability and DNA hypermethylation. *Cancer Cell*. 2012;22(5):645–655.
56. Tallerico R, et al. IL-15, TIM-3 and NK cells subsets predict responsiveness to anti-CTLA-4 treatment in melanoma patients. *Oncoimmunology*. 2017;6(2):e1261242.
57. Delconte RB, et al. CIS is a potent checkpoint in NK cell-mediated tumor immunity. *Nat Immunol*. 2016;17(7):816–824.
58. Sungur CM, et al. Murine natural killer cell licensing and regulation by T regulatory cells in viral responses. *Proc Natl Acad Sci USA*. 2013;110(18):7401–7406.
59. Hallett WHD, et al. Combination therapy using IL-2 and anti-CD25 results in augmented natural killer cell-mediated antitumor responses. *Biol Blood Marrow Transplant*. 2008;14(10):1088–1099.
60. Alvarez M, Sungur CM, Ames E, Anderson SK, Pomeroy C, Murphy WJ. Contrasting effects of anti-Ly49A due to MHC class I cis binding on NK cell-mediated allogeneic bone marrow cell resistance. *J Immunol*. 2013;191(2):688–698.
61. Hesslein DG, Takaki R, Hermiston ML, Weiss A, Lanier LL. Dysregulation of signaling pathways in CD45-deficient NK cells leads to differentially regulated cytotoxicity and cytokine production. *Proc Natl Acad Sci USA*. 2006;103(18):7012–7017.